DTU Library

All-optical wavelength conversion and signal regeneration using an electroabsorption modulator

Højfeldt, Sune; Bischoff, Svend; Mørk, Jesper

Published in:
Proceedings of LEOS'99 Annual Meeting

Link to article, DOI:
10.1109/LEOS.1999.811968

Publication date:
1999

Document Version
Publisher's PDF, also known as Version of record

11:30am - 11:45am

ThO4

All-optical wavelength conversion and signal regeneration using an electroabsorption modulator

S. Højfeldt (1), S. Bischoff, J. Mørk

Research Center COM

Technical University of Denmark, Building 349, DK-2800 Lyngby, Denmark

(1) email: sh@com.dtu.dk

Abstract: All-optical wavelength conversion in an InGaAsP quantum well electroabsorption modulator is studied at different bit-rates. We present theoretical results showing wavelength conversion efficiency in agreement with existing experimental results, and signal regeneration capability is demonstrated.

Introduction

Recently, the use of electroabsorption modulators (EAMs) for all-optical signal processing has been demonstrated experimentally. Wavelength conversion at up to 40 Gbit/s was performed with good performance up to 20 Gbit/s [1]. The conversion in an EAM relies on the saturable absorption characteristic, through cross-absorption modulation. Note that this avoids the inversion, which results when using cross-gain modulation in semiconductor optical amplifiers [2]. Signal regeneration at 10 Gbit/s has also been demonstrated [3]. The regenerative capability of the EAM relies on saturation of the absorption by the incoming signal itself.

We present theoretical results that are in good agreement with the experimental results, and demonstrate explicitly the importance of device length and input power level on the conversion results. It is also shown that the material recovery time must meet strict demands to provide reasonable performance at 40 Gbit/s.

Theory

We use a large-signal model for a reverse-biased quantum well absorber originally designed to study colliding-pulse mode-locked lasers [4]. It includes propagation effects and a detailed gain model. Ultra-fast effects such as spectral hole burning and two-photon absorption are also taken into account. Further, we include a simple, carrier dependent sweep-out time. The sweep-out time increases at high carrier densities due to a screening of the internal field. Sweep-out times on the order of several tens of picoseconds in multi quantum-well InGaAsP and AlGaAs structures have been found, even at relatively high reverse biases, around –5 V [5, 6]. Based on the results in [1], we have assumed that the sweep-out time varying from 10 to 25 ps.

Wavelength conversion and signal regeneration at 10 Gbit/s

To demonstrate the wavelength conversion and signal regeneration capability of the EAM to provide wavelength conversion as well as signal improvement, we propagate various bit patterns consisting of 8 ps wide pulses with an extinction ratio (*ER*) of 10 dB (peak-to-floor) through the device.

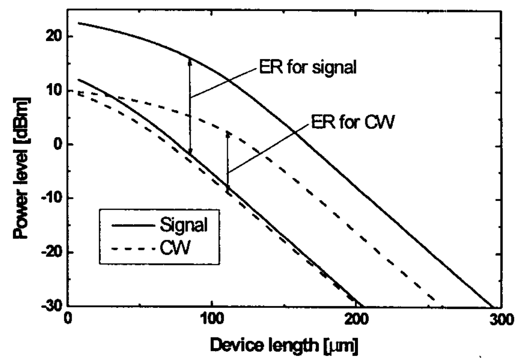

Figure 1: Power levels for space ("0") and mark ("1") as function of length for signal and CW. The bit rate is 10 Gbit/s.

Figure 1 shows a simulation where a 10 dBm CW signal ("CW") at 1520 nm and a 14.5 dBm average pulse power bit-stream signal ("signal") at 1510 nm are launched into an EAM from the same end (co-propagating scheme). In practice, the two signals would be separated at the output of the device using a spectral filter. The figure shows the power levels for "mark" and "space" as a function of device length. As the length increases, the *ER* for both signal and CW increase, demonstrating both the wavelength conversion and reshaping capabilities of the device. When the remaining power level becomes too low to influence significantly the carrier density, the *ER* values become constant. All in all, the figure clearly shows that the improvement in *ER* comes about due to the non-linear saturation properties: The energy in the "0" decreases more rapidly than the energy in a "1" due to a higher absorption for smaller input power levels. In order to ensure a certain power level at the output (e.g., 10 dB above the ASE level in an amplifier), the length must be below a certain value, which of course depends on the input power levels.

Pulse energy dependence

The obtainable *ER* depends on the input power of the signal. Figure 2 shows the *ER* as a function of device length for various pulse energies. Corresponding to an average power of 11.5 dBm, an *ER* of ~10 can be obtained on the converted signal. Past this point, the *ER* can not be improved further because the signal is too weak to bleach the absorption, but the power level of course keeps

0-7803-5634-9/99/$10.00©1999 IEEE

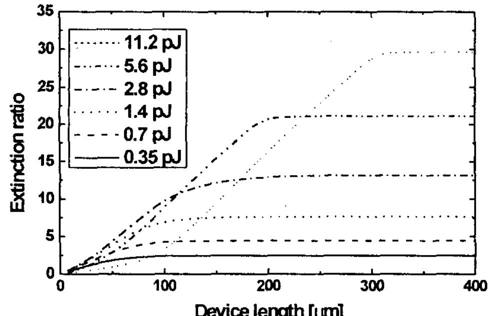

Figure 2: Extinction ratio of converted signal as function of length with input pulse energy as a parameter

decreasing due to absorption. Therefore, it is desirable to operate the device up to, but not beyond the point where the *ER* levels out. Figure 2 shows that the *ER* obtained below, say, 150 µm, for the highest input power level is smaller than that obtained using lower input power levels. This is because the saturation of the absorption in the first part of the device suppresses efficient carrier density modulation, indicating that for a certain device length there is an optimum input power level giving the highest *ER* at the output of the device.

Wavelength conversion up to 40 Gbit/s

To investigate the capability of the EAM to perform wavelength conversion at higher bit-rates, we modelled the propagation of 20 and 40 Gbit/s pulsetrains through the EAM. Again, we chose pulsetrains that ensured that a worst-case scenario (in terms of eye-distortion) was described.

The eye-diagrams for different EAM lengths of 125 and 200 µm are shown for different power levels in Fig. 3 and Fig. 4. The signal power levels for the 10, 20 and 40 Gbit/s signals in Fig.3 (Fig.4) were 11, 16 (19) and 19 (22) dBm, respectively.

In Fig. 3, the quality of the eye for the 10 Gbit/s signal does not improve from 125 to 200 µm, because the power level is too small (see also Fig. 2). For the 20 Gbit/s signal, the eye-quality in Fig. 3 is seen to improve

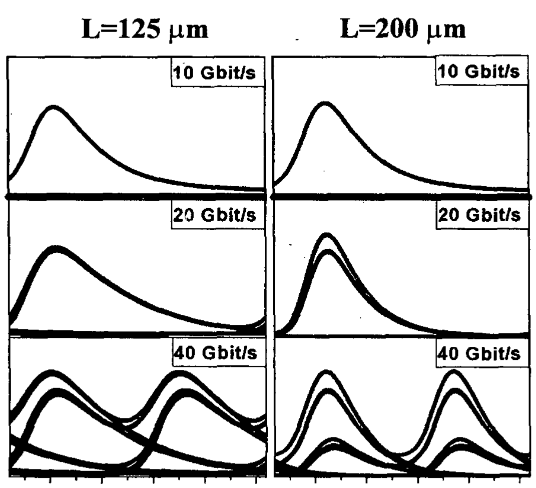

Figure 2: Eye-diagrams for converted signals at 10, 20 and 40 Gbit/s. The average input power level is 11, 16 and 19 dBm, respectively.

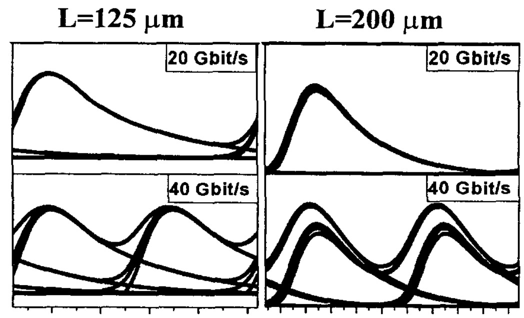

Figure 3: Eye-diagrams for converted signals at 20 and 40 Gbit/s. The average input power level is 19 and 22 dBm, respectively.

significantly as the length of the EAM is increased. Finally, the 40 Gbit/s signal eye-quality decreases for the long EAM. The difference in observed conversion efficiency is due to the saturable recovery time, which is a severe limitation for obtaining good wavelength conversion efficiency at high bit rates. The distortion in the 40 Gbit/s eye arises when the power levels in each "mark" can no longer sufficiently saturate the absorber. Immediately following marks will then experience less absorption, giving rise to the distortion. These results agree well with the experimental results in [1]. In Fig.4, where the power level is twice as large, this distortion is suppressed due to the higher power level after 200 µm, resulting in a better eye-quality. The eye for 20 Gbit/s, where the same effect takes place to a smaller degree, also improves correspondingly from Fig.3 to Fig. 4 (200 µm).

Conclusion

We have modelled wavelength conversion and signal regeneration using an electroabsorption modulator. A critical dependence of the conversion efficiency on device length and input power levels was demonstrated and explained. Also, it is critical for the operation of the device at high speeds that the recovery time is low, at most equal to the timeslot available at the given bit-rate. The extinction ratio is shown to saturate at a level, which increases with the signal input power at bit rates up to 20 Gbit/s. At 40 Gbit/s the resulting eye of the converted signal is critically dependent on the absorber length and the injected power.

References

[1] N. Edagawa, M. Suzuki, S. Yamamoto, IEICE Trans. Electron., **E81-C**, 1251 (1998).

[2] T. Durhuus, B. Mikkelsen, C. Joergensen, S. L. Danielsen, K. E. Stubkjaer. J. Lightwave Technol., **14**, 942 (1996).

[3] H. Yokoyama, Y. Hashimoto, H. Kurita. Techn. Digest CLEO'98., **6**, 502 (1998).

[4] S. Bischoff, J. Mørk, T. Franck, S. D. Brorson, M. Hofmann, K. Fröjdh, L. Prip, M. P. Sørensen, Quantum Semiclass. Opt., **9**, 655 (1997).

[5] J.A. Cavaillès, D.A.B. Miller, J.E. Cunningham, P. Li Kam Wa, A. Miller, IEEE J. Quantum Electron., **28**, 2486 (1992).

[6] P. J. Bradley, C. Rigo, A. Stano, IEEE J. Quantum Electron., **32**, 43 (1996).